Title: Nardilysin promotes hepatocellular carcinoma through activation of signal transducer and activator of transcription 3

Authors' names: Yosuke Kasai[1], Kan Toriguchi[1,2], Etsuro Hatano[1,3], Kiyoto Nishi[4], Mikiko Ohno[4], Tomoaki Yoh[1], Keita Fukuyama[1], Takahiro Nishio[1], Masayuki Okuno[1], Keiko Iwaisako[5], Satoru Seo[1], Kojiro Taura[1], Masato Kurokawa[6], Makoto Kunichika[6], Shinji Uemoto[1], Eiichiro Nishi[4,7]

Yosuke Kasai and Kan Toriguchi contributed equally to this work

Authors' affiliations: [1] Department of Surgery, Graduate School of Medicine, Kyoto University, Kyoto, Japan, [2] Department of Surgery, Helen Diller Family Comprehensive Cancer Center, University of California San Francisco, CA, USA, [3] Department of Surgery, Hyogo College of Medicine, Nishinomiya, Japan, [4] Department of Cardiovascular Medicine, Graduate School of Medicine, Kyoto University, Kyoto, Japan, [5] Department of Target Therapy and Oncology, Graduate School of Medicine, Kyoto University, Kyoto, Japan, [6] Sanyo Chemical Industries Ltd., Kyoto, Japan, [7] Department of Pharmacology, Shiga University of Medical Science, Otsu, Japan

Addresses:

[1, 4, 5] 54 Kawaharacho Shogoin, Sakyo-ku, Kyoto, 6068507, Japan, [2] 2340 Sutter Street, San Francisco, CA, 94143, USA, [3] 1-1 Mukogawa-cho, Nishinomiya, Hyogo, 6638501, Japan, [6] 11-1, Ikkyo Nomoto-cho, Higashiyama-ku, Kyoto, 6050995, Japan, [7] Seta Tsukinowa-cho, Otsu, Shiga, 5202192, Japan

Corresponding author:

Eiichiro Nishi, MD, PhD

Department of Cardiovascular Medicine, Graduate School of Medicine, Kyoto University

54 Kawaharacho Shogoin, Sakyo-ku, Kyoto, 6068507, Japan

TEL: +81 75 751 3187, FAX: +81 75 751 3203

E-mail: nishi@kuhp.kyoto-u.ac.jp

Department of Pharmacology, Shiga University of Medical Science

Seta Tsukinowa-cho, Otsu, Shiga, 5202192, Japan

TEL: +81 77 548 2181, FAX: +81 77 548 2183

E-mail: enishi@belle.shiga-med.ac.jp

and

Etsuro Hatano, MD, PhD

Department of Surgery, Hyogo College of Medicine

1-1 Mukogawa-cho, Nishinomiya, Hyogo, 6638501, Japan

TEL: +81 798 45 6582, FAX: +81 798 45 6581

E-mail: shatano@hyo-med.ac.jp

Word counts: 4126 words

Number of tables/figures: 2/4

Quantity of supporting information: 2 supplementary figures and 2 supplementary tables

Abstract (228 words)

Nardilysin (NRDC) is a metalloendopeptidase of the M16 family. We previously showed that NRDC activates inflammatory cytokine signaling, including interleukin-6-signal transducer and activator of transcription 3 (STAT3) signaling. NRDC has been implicated in the promotion of breast, gastric, and esophageal cancer, as well as the development of liver fibrosis. In this study, we investigated the role of NRDC in the promotion of hepatocellular carcinoma (HCC), both clinically and experimentally. We found that NRDC expression was up-regulated 3-fold in HCC tissue compared to the adjacent non-tumor liver tissue, which was confirmed by immunohistochemistry and western blotting. We also found that high serum NRDC was associated with large tumor size (> 3 cm, $P = 0.016$) and poor prognosis after hepatectomy (median survival time 32.0 vs. 73.9 months, $P = 0.003$) in patients with hepatitis C (n = 120). Diethylnitrosamine-induced hepatocarcinogenesis was suppressed in heterozygous NRDC-deficient mice compared to their wild-type littermates. Gene silencing of NRDC with miRNA diminished the growth of Huh-7 and Hep3B spheroids *in vitro*. Notably, phosphorylation of STAT3 was decreased in NRDC-depleted Huh-7 spheroids compared to control spheroids. The effect of a STAT3 inhibitor (S3I-201) on the growth of Huh-7 spheroids was reduced in NRDC-depleted cells relative to controls. Our results show

that NRDC is a promising prognostic marker for HCC in patients with hepatitis C, and that NRDC promotes tumor growth through activation of STAT3.

Keywords: hepatocellular carcinoma, nardilysin, prognostic marker, signal transducer and activator of transcription 3, spheroid

Abbreviations

CART: classification and regression tree

DEN: diethylnitrosamine

FPKM-UQ: upper quartile fragments per kilobase of exon per million reads mapped

HB-EGF: heparin-binding epidermal growth factor-like growth factor

HBs-antigen: hepatitis B surface antigen

HCC: hepatocellular carcinoma

HCV: hepatitis C virus

NC: negative control

NRDC: nardilysin (N-arginine dibasic convertase)

STAT3: signal transducer and activator of transcription 3

TCGA: The Cancer Genome Atlas

TNF-α: tumor necrosis factor-alpha

Introduction

Hepatocellular carcinoma (HCC) is one of the most common cancers and the third leading cause of cancer-related deaths worldwide.[1] Low-grade inflammation, induced by chronic hepatitis B and C and steatohepatitis, is the established pathogen of HCC,[2] but much remains to be learned about how HCC initiates and progresses. The long-term prognosis of HCC, even after curative surgical resection or percutaneous ablation therapy, is unsatisfactory because of the high incidence of recurrence, with a 3- and 5-year recurrence rate of more than 50% and 70%, respectively.[3-5] Although sorafenib, a multi-kinase inhibitor, has been established as the standard therapy for advanced HCC,[5] even with such treatment, the prognosis for advanced HCC remains dismal with a median survival time of less than 1 year.[6] Identification of novel therapeutic targets for HCC is urgently needed.

Nardilysin (N-arginine dibasic convertase = NRDC) is a metalloendopeptidase of the M16 family. We first identified NRDC as a specific binding protein of the heparin-binding epidermal growth factor-like growth factor (HB-EGF).[7] Thereafter, we showed that NRDC enhances ectodomain shedding of HB-EGF and other membrane proteins including tumor necrosis factor-alpha (TNF-α).[8-10] In addition to its functions at the cell surface, nuclear functions of NRDC as a transcriptional co-regulator have

been identified.[11-13] NRDC has been implicated in the promotion of breast,[14] gastric,[10] and esophageal cancer.[15] In gastric cancer, we demonstrated that NRDC promotes cancer cell proliferation via activation of an interleukin-6-signal transducer and activator of transcription 3 (STAT3) pathway that was induced by the enhancement of TNF-α shedding. We reported that NRDC also promotes liver fibrosis in mice via TNF-α signaling.[16]

In the present study, we investigated the role of NRDC in the promotion of HCC, both clinically and experimentally, and explored whether NRDC might be a prognostic marker and therapeutic target for HCC.

Materials and Methods

Patients and clinical samples

For measurement of serum NRDC, preoperative serum samples were obtained from 220 of 685 patients who underwent hepatectomy for HCC between 1996 and 2006 at the Department of Surgery, Kyoto University Hospital. As a control group, serum samples were obtained from 112 healthy volunteers who had been shown not to have any malignant disorder. Serum NRDC was measured using an ELISA, as previously described.[10] Kaplan-Meier analysis was used to assess the prognostic impact of serum NRDC on overall survival, recurrence-free survival, and survival after recurrence. Resected specimens were either preserved as separate fresh-frozen blocks of the tumor and adjacent non-tumor liver tissue, or fixed in 10% formalin (Wako, Osaka, Japan) and embedded in paraffin for immunohistochemistry. Written informed consent was obtained from all patients. This study was performed in accordance with the Declaration of Helsinki and the Japanese ethical guidelines for epidemiological research and was approved by the Kyoto University Graduate School and Faculty of Medicine, Ethics Committee (Approval code: E1840 and R0571).

Cohort study from The Cancer Genome Atlas database

HCC data from The Cancer Genome Atlas (TCGA) was downloaded from the Broad Institute's Firehose pipeline using the RTCGAToolbox.[17] We integrated clinical data and upper quartile normalized RNAseqv2 data from cancer tissue. The breakpoint of log2-transformed upper quartile fragments per kilobase of exon per million reads mapped (FPKM-UQ) of the NRDC gene was determined by the classification and regression tree (CART) technique.[18] For analysis of the TCGA database, R and the Bioconductor survival,[19] party,[18] MASS,[20] stringr,[21] and RTCGAToolbox packages were used.

Mice and the hepatocarcinogenesis model

Heterozygous NRDC-deficient mice (*Nrdc* +/-) (Accession No. CDB0466K, http://www.clst.riken.jp/arg/mutant%20mice%20list.html) on a C57BL/6 background were used along with wild-type littermates.[22] Mice were maintained in filter-topped cages and fed an autoclaved diet of regular chow and tap water according to the guidelines of the Institutional Animal Care and Use Committee of Kyoto University. In the diethylnitrosamine (DEN, Sigma-Aldrich, St. Louis, MO, USA)-induced hepatocarcinogenesis model, DEN (25 mg/kg) was injected intraperitoneally into mice once on day 14 after birth.[23] Mice were sacrificed at 36 weeks of age and liver tissue

was collected and rapidly fixed in 10% formalin for immunochemical analysis.

Cell lines, reagents, and stable knockdown of NRDC and STAT3

Human HCC cell lines, Huh-7 and Hep3B, were cultured in DMEM (Thermo Fisher, Scientific, Waltham, MA, USA) supplemented with 10% FBS and 1% penicillin/streptomycin under 5% CO2 at 95% humidity and 37 °C. Gene knockdown of NRDC or STAT3 in Huh-7 and Hep3B cells was performed by transduction of lentiviral vectors expressing miRNA, as previously described.[10] Target sequences were: miR-NRDC-1, 5′-CTGATGCAAACAGAAAGGAAA-3′; miR-NRDC-2, 5′-GAGAAATGGTTTGGAACTCAA-3′; miR-STAT3-1, 5'-CCAATGGAGATTGCCCGGATT-3'; miR-STAT3-2, 5'-TTGTGGTGATCTCCAACATCT-3'. We used a control vector that contains a non-targeting sequence for any vertebrate gene as a negative control (NC).

Multicellular spheroid growth assay

Huh-7 and Hep3B cells were seeded into 96-well round bottom ultra-low attachment microplates (Corning, NY, USA) at densities of 1,000 cells and 2,500 cells, respectively, in 200 μl of growth medium supplemented with 10% FBS per well. The

cells were allowed to spontaneously aggregate, as described previously.[24] Spheroids were observed with an inverted microscope (Keyence, Osaka, Japan) and the sectional area [S (×10,000 μm^2)] of each spheroid was measured with Image J software (NIH, Bethesda, MD, USA). The volume index of the spheroid was calculated as $S^{1.5}$.

Spheroid growth inhibition assay

S3I-201 (a small molecule STAT3 inhibitor, Santa Cruz Biotechnology, Dallas, TX, USA), dissolved in DMSO (Wako), was added to growth medium supplemented with 10% FBS immediately after cell seeding into 96-well ultra-low attachment microplates. Equivalent amounts of DMSO were used as the control for S3I-201. The effect of S3I-201 on spheroid growth was evaluated after 7 days of treatment.

Immunohistochemistry

Immunohistochemistry was performed as previously described.[10] Four-μm thick sections were incubated with the indicated primary antibody (4 °C overnight): anti-human NRDC mouse monoclonal antibody (#102, established in our laboratory) for human liver specimens, dilution 1:500; anti-mouse NRDC rat monoclonal antibody (#135, established in our laboratory) for mouse liver specimens, dilution 1:200; and Ki67

(DakoCytomation, Glostrup, Denmark) for mouse liver specimens, dilution 1:100. Human specimens were incubated with mouse Envision polymer (DAKO) at room temperature for 1 hour. Mouse specimens were incubated with biotinylated secondary antibody for 1-2 hours and then with the avidin-biotin-peroxidase complex (Vectastain ABC kit, Vector Laboratories, Burlingame, CA, USA) at room temperature for 30 minutes.

Western blotting

Western blotting was performed as previously described.[13] Twenty μg of tissue lysate, or 10 μg of cell lysate isolated from spheroids, was electrophoresed on a 10% SDS-polyacrylamide gel (SDS from Wako; acrylamide from Bio Rad, Hercules, CA, USA) and transferred to a nitrocellulose membrane (GE Healthcare, Buckinghamshire, UK). The targets of the primary antibodies are listed in Table S1. The blot was observed with EZ-Capture II software (ATTO, Tokyo, Japan) after being visualized by ECL Prime (GE Healthcare). Analysis of densitometry was performed using Image J software.

Statistical analysis

Continuous variables were expressed as the median or the mean plus/minus

the standard error, and compared using Wilcoxon's test, or the paired or unpaired t-test, as appropriate. Categorical variables were compared using the chi-squared test. The optimal cutoff value of serum NRDC that defined the prognosis of HCC was determined according to receiver operating characteristic analysis for the outcome of death within 3 years of surgery. Cumulative survival rates were calculated using the Kaplan-Meier method and compared using the log-rank test. Multivariate analysis for overall survival was performed using the Cox proportional hazard model. A two-tailed P value less than 0.05 was considered to be significant. Statistical analyses were performed using JMP software version 10 (SAS Institute Inc., Cary, NC, USA).

Results

NRDC is up-regulated in HCC tissue and serum NRDC is a prognostic marker for HCC patients with hepatitis C

Immunohistochemistry using an anti-NRDC antibody revealed that NRDC expression was higher in HCC compared to the adjacent non-tumor liver tissue (Fig. 1a). This finding was confirmed by western blot analysis, which showed that NRDC expression was up-regulated 3-fold in HCC compared to the adjacent non-tumor liver tissue (Fig. 2b and 2c). Serum NRDC was 1.7 times higher in HCC patients compared to healthy volunteers (median 934.1 vs. 539.8 pg/ml, respectively, $P < 0.001$, Fig. 1d), and correlated modestly, but positively, with the tumor to non-tumor ratio of histological NRDC expression (Fig. 1e). These results suggest that the systemic concentration of NRDC reflects the amount of NRDC in cancer tissues. Serum NRDC did not correlate with tumor multiplicity, vascular invasion, or background liver cirrhosis, but did correlate with tumor size and extrahepatic metastasis (Table 1 and Table S2). Overall survival for all patients was not associated with serum NRDC (Fig. S1a). However, among patients with hepatitis C (n = 120), overall survival was significantly shorter in patients with high serum NRDC than in those with low serum NRDC (median survival time 32.0 vs. 73.9 months, respectively, $P = 0.003$, Fig. 1f). Interestingly, survival after

recurrence, rather than recurrence-free survival, differed significantly between patients with high serum NRDC levels and those with low serum NRDC (median survival time 27.8 vs. 49.0 months, respectively, $P = 0.023$, Fig. 1g, 1h, and S1b, S1c). In multivariate analysis among patients with hepatitis C, high serum NRDC was an independent prognostic factor for overall survival (Table 2). Thus, high expression of NRDC in cancer tissues correlates with poor prognosis for HCC patients with hepatitis C. Consistent with our observations, survival analysis using the TCGA database showed that high NRDC gene expression in HCC was associated with poor prognosis (Fig. S2a and S2b). These findings strongly suggest that NRDC is a prognostic marker for HCC in patients with hepatitis C.

DEN-induced hepatocarcinogenesis is suppressed in NRDC-deficient mice

To determine the involvement of NRDC in the pathogenesis of HCC, DEN-induced hepatocarcinogenesis, a well-established mouse model of HCC, was examined in NRDC-deficient mice. As homozygous deficient mice show multiple phenotypes, including growth retardation and hypothermia,[12, 22] we used heterozygous deficient (*Nrdc* +/-) mice for our experiments. Hepatocarcinogenesis was suppressed in *Nrdc* +/- mice compared to *Nrdc* +/+ mice, as assessed by macroscopic tumor number

and maximum tumor size (Fig. 2a). As in human HCC, NRDC was up-regulated in the liver tumor compared to the adjacent non-tumor tissue, even in *Nrdc* +/- mice (Fig. 2b). The proportion of Ki67-positive proliferating cells was significantly lower in the livers of *Nrdc* +/- mice compared to the livers of *Nrdc* +/+ mice (Fig. 2c). These results indicate that NRDC expression correlates positively with tumor cell proliferation.

Gene knockdown of NRDC suppresses spheroid growth and STAT3 phosphorylation in HCC cells

To explore the function of NRDC in HCC cells, NRDC was stably knocked-down using miRNA in Huh-7 and Hep3B cells from which spheroids were developed, as described in the Methods. Three-dimensional multicellular spheroid growth assays then demonstrated that gene silencing of NRDC suppressed Huh-7 and Hep3B spheroid growth (Fig. 3a and 3b). Of note, phosphorylation of STAT3 at tyrosine 705 was significantly decreased in spheroids of NRDC-knockdown Huh-7 cells (Fig. 3c). STAT3 is one of the key promoters of HCC,[25] and we previously showed that NRDC induces STAT3 phosphorylation in gastric cancer cells.[10] To confirm the role of STAT3 in spheroid growth, we established Huh-7 cells stably transduced with a lentiviral vector expressing miRNA against STAT3. Knockdown of STAT3 decreased STAT3

phosphorylation (Fig. 4a) and suppressed spheroid growth (Fig. 4b). Furthermore, a small molecule STAT3 inhibitor (S3I-201) was less effective in affecting spheroid growth in NRDC-knockdown than control cells (Fig. 4c), which indicates that NRDC regulates spheroid growth via STAT3 activation.

Discussion

In this study, we investigated whether NRDC contributes to the promotion of HCC, both clinically and experimentally, and explored the potential of NRDC as a prognostic marker and therapeutic target for HCC. Our results show that 1) NRDC is up-regulated in HCC tissue; 2) high serum NRDC is associated with increased tumor size and poor prognosis among patients with hepatitis C; 3) DEN-induced hepatocarcinogenesis is suppressed in NRDC-deficient mice; and 4) NRDC promotes the growth of HCC spheroids via activation of STAT3.

Our results suggest that NRDC could be a useful prognostic marker for HCC in patients with hepatitis C because of its ability to predict survival time after recurrence; this capacity of NRDC is unlike that of other markers which predict overall survival or recurrence after curative treatment for HCC.[26-28] Survival time after recurrence depends on the pattern of recurrence, including the tumor number and size for intrahepatic recurrence and the presence or absence of extrahepatic spread. It also depends on the efficacy of the curative treatment for recurrent lesions.[29-31] Although serum NRDC at the time of surgery was not associated with the time to recurrence, we suggest that this value could be associated with the aggressive tumor properties that persist after recurrence. This finding could alter postoperative surveillance; more

intensive surveillance could be scheduled in the patients with high serum NRDC at the time of surgery for the early detection and treatment of recurrent lesions.

We showed that deletion or gene silencing of NRDC diminished tumor size in a mouse model of HCC *in vivo* and spheroid growth *in vitro*. The association between serum NRDC and tumor size in the clinical data is consistent with these results. We used a 3-dimensional spheroid growth assay to evaluate *in vitro* cell growth, because 3-dimensional cell culture mimics the *in vivo* tumor characteristics better than 2-dimensional cell culture in terms of cell-cell interactions, oxygen and chemical gradients, and gene expression profiles.[24] In the analysis of signal transduction in HCC cells derived from spheroids, gene silencing of NRDC decreased phosphorylation of STAT3. STAT3 is one of the key promoters of HCC and regulates the transcription of genes involved in cell proliferation, epithelial-to-mesenchymal transition, angiogenesis, and metastasis.[25, 32-34] STAT3 is also associated with “stemness” and spheroid formation.[35, 36] In this study, we also show that inhibition of STAT3 suppressed spheroid growth and NRDC-knockdown cells were less dependent on STAT3 signaling for spheroid growth. These data indicate that spheroid growth promoted by NRDC is, at least partially, mediated by activation of STAT3. This result is compatible with our previous findings on gastric cancer, showing that NRDC activates STAT3.[10]

NRDC has many functions which are dependent on its cellular localization including activation of ectodomain shedding on the cell surface,[8-10, 22, 37] and protease activity in the cytoplasm.[38] In addition, the nuclear functions of NRDC as a transcriptional co-regulator have been described.[11-13] Our preliminary results of chromatin immunoprecipitation sequence analysis suggest that NRDC and STAT3 co-localize on the genome of mouse liver tissue. This finding suggests that NRDC may interact with STAT3 and regulate the activity of STAT3.

Our clinical data suggest that NRDC promotes HCC in a hepatitis C virus (HCV)-specific manner. Accumulated evidence suggests a relationship between HCV infection and activation of STAT3. Replication of HCV generates oxidative stress in host cells, resulting in the constitutive activation of STAT3.[39-41] Direct interaction of the HCV core protein and STAT3 leads to cellular transformation.[42, 43] Moreover, the HCV core protein facilitates the epithelial-to-mesenchymal transition of HCC cells through STAT3 activation.[34] These findings indicate that HCV is involved in both the initiation and promotion of HCC in a STAT3 dependent manner. Together, NRDC and HCV affect HCC through activation of STAT3. Given the positive correlation of serum NRDC and poor prognosis in HCC patients with hepatitis C, NRDC, in association with HCV, might promote the aggressiveness of HCC via STAT3 activation, although further study would

be required to confirm this speculation.

In conclusion, NRDC is a novel and unique prognostic marker that predicts survival after recurrence as well as overall survival for HCC in patients with hepatitis C. Also, NRDC promotes tumor growth, at least in part, through activation of STAT3, suggesting that NRDC could be a therapeutic target for HCC.

Acknowledgements

This study was supported by Grants-in-Aid KAKENHI (26293068, 15K19513, 15K19376, 15H01557, 16K15216). It was also supported by the Takeda Science Foundation, The Uehara Memorial Foundation, The Kanae Foundation for the Promotion of Medical Science, and The MSD Life Science Foundation. We thank Prof. D. Donner, from the University of California San Francisco, for editing the manuscript.

Disclosure

The authors have no conflict of interest.

References

1 Ferlay J, Shin HR, Bray F, Forman D, Mathers C, Parkin DM. Estimates of worldwide burden of cancer in 2008: GLOBOCAN 2008. *Int J Cancer* 2010; **127**: 2893-917.

2 McGlynn KA, London WT. The global epidemiology of hepatocellular carcinoma: present and future. *Clin Liver Dis* 2011; **15**: 223-43, vii-x.

3 Belghiti J, Panis Y, Farges O, Benhamou JP, Fekete F. Intrahepatic recurrence after resection of hepatocellular carcinoma complicating cirrhosis. *Ann Surg* 1991; **214**: 114-7.

4 Poon RT, Fan ST, Lo CM et al. Extended hepatic resection for hepatocellular carcinoma in patients with cirrhosis: is it justified? *Ann Surg* 2002; **236**: 602-11.

5 Liver EAFTSOT, Cancer EOFRATO. EASL-EORTC clinical practice guidelines: management of hepatocellular carcinoma. *J Hepatol* 2012; **56**: 908-43.

6 Llovet JM, Ricci S, Mazzaferro V et al. Sorafenib in advanced hepatocellular carcinoma. *N Engl J Med* 2008; **359**: 378-90.

7 Nishi E, Prat A, Hospital V, Elenius K, Klagsbrun M. N-arginine dibasic convertase is a specific receptor for heparin-binding EGF-like growth factor that mediates cell migration. *EMBO J* 2001; **20**: 3342-50.

8 Nishi E, Hiraoka Y, Yoshida K, Okawa K, Kita T. Nardilysin enhances ectodomain

shedding of heparin-binding epidermal growth factor-like growth factor through activation of tumor necrosis factor-alpha-converting enzyme. *J Biol Chem* 2006; **281**: 31164-72.

9 Hiraoka Y, Yoshida K, Ohno M, Matsuoka T, Kita T, Nishi E. Ectodomain shedding of TNF-alpha is enhanced by nardilysin via activation of ADAM proteases. *Biochem Biophys Res Commun* 2008; **370**: 154-8.

10 Kanda K, Komekado H, Sawabu T et al. Nardilysin and ADAM proteases promote gastric cancer cell growth by activating intrinsic cytokine signalling via enhanced ectodomain shedding of TNF-α. *EMBO Mol Med* 2012; **4**: 396-411.

11 Li J, Chu M, Wang S et al. Identification and characterization of nardilysin as a novel dimethyl H3K4-binding protein involved in transcriptional regulation. *J Biol Chem* 2012; **287**: 10089-98.

12 Hiraoka Y, Matsuoka T, Ohno M et al. Critical roles of nardilysin in the maintenance of body temperature homoeostasis. *Nat Commun* 2014; **5**: 3224.

13 Nishi K, Sato Y, Ohno M et al. Nardilysin Is Required for Maintaining Pancreatic ß-Cell Function. *Diabetes* 2016; **65**: 3015-27.

14 Choong LY, Lim SK, Chen Y et al. Elevated NRD1 metalloprotease expression plays a role in breast cancer growth and proliferation. *Genes Chromosomes Cancer* 2011; **50**: 837-47.

15 Uraoka N, Oue N, Sakamoto N et al. NRD1, which encodes nardilysin protein, promotes esophageal cancer cell invasion through induction of MMP2 and MMP3 expression. *Cancer Sci* 2014; **105**: 134-40.

16 Ishizu-Higashi S, Seno H, Nishi E et al. Deletion of nardilysin prevents the development of steatohepatitis and liver fibrotic changes. *PLoS One* 2014; **9**: e98017.

17 Samur MK. RTCGAToolbox: a new tool for exporting TCGA Firehose data. *PLoS One* 2014; **9**: e106397.

18 Hothorn T, Hornik K, Zeileis A. Unbiased recursive partitioning: A conditional inference framework. *J Comp Graph Stat* 2006; **15**: 651-74.

19 Therneau T, Grambsch P. Modeling survival data: extending the Cox model. New York: Springer Science & Business Media, 2000.

20 Ripley W. Modern Applied Statistics With S. New York: Springer, 2002.

21 Wickham H. Stringr: Simple, consistent wrappers for common string operations. R package version 1. 2015.

22 Ohno M, Hiraoka Y, Matsuoka T et al. Nardilysin regulates axonal maturation and myelination in the central and peripheral nervous system. *Nat Neurosci* 2009; **12**: 1506-13.

23 Vesselinovitch SD, Mihailovich N. Kinetics of diethylnitrosamine hepatocarcinogenesis in the infant mouse. *Cancer Res* 1983; **43**: 4253-9.

24 Vinci M, Gowan S, Boxall F et al. Advances in establishment and analysis of three-dimensional tumor spheroid-based functional assays for target validation and drug evaluation. *BMC Biol* 2012; **10**: 29.

25 He G, Karin M. NF-κB and STAT3 - key players in liver inflammation and cancer. *Cell Res* 2011; **21**: 159-68.

26 Budhu A, Roessler S, Zhao X et al. Integrated metabolite and gene expression profiles identify lipid biomarkers associated with progression of hepatocellular carcinoma and patient outcomes. *Gastroenterology* 2013; **144**: 1066-75.e1061.

27 Tao YM, Huang JL, Zeng S et al. BTB/POZ domain-containing protein 7: epithelial-mesenchymal transition promoter and prognostic biomarker of hepatocellular carcinoma. *Hepatology* 2013; **57**: 2326-37.

28 Jin GZ, Yu WL, Dong H et al. SUOX is a promising diagnostic and prognostic biomarker for hepatocellular carcinoma. *J Hepatol* 2013; **59**: 510-7.

29 Poon RT, Fan ST, Lo CM, Liu CL, Wong J. Long-term survival and pattern of recurrence after resection of small hepatocellular carcinoma in patients with preserved liver function: implications for a strategy of salvage transplantation. *Ann Surg* 2002; **235**: 373-82.

30 Minagawa M, Makuuchi M, Takayama T, Kokudo N. Selection criteria for repeat hepatectomy in patients with recurrent hepatocellular carcinoma. *Ann Surg* 2003; **238**:

703-10.

31 Taura K, Ikai I, Hatano E, Fujii H, Uyama N, Shimahara Y. Implication of frequent local ablation therapy for intrahepatic recurrence in prolonged survival of patients with hepatocellular carcinoma undergoing hepatic resection: an analysis of 610 patients over 16 years old. *Ann Surg* 2006; **244**: 265-73.

32 Li WC, Ye SL, Sun RX et al. Inhibition of growth and metastasis of human hepatocellular carcinoma by antisense oligonucleotide targeting signal transducer and activator of transcription 3. *Clin Cancer Res* 2006; **12**: 7140-8.

33 Zhang JF, He ML, Fu WM et al. Primate-specific microRNA-637 inhibits tumorigenesis in hepatocellular carcinoma by disrupting signal transducer and activator of transcription 3 signaling. *Hepatology* 2011; **54**: 2137-48.

34 Zhou JJ, Meng Z, He XY et al. Hepatitis C virus core protein increases Snail expression and induces epithelial-mesenchymal transition through the signal transducer and activator of transcription 3 pathway in hepatoma cells. *Hepatol Res* 2016 doi: 10.1111/hepr.12771

35 Wan S, Zhao E, Kryczek I et al. Tumor-associated macrophages produce interleukin 6 and signal via STAT3 to promote expansion of human hepatocellular carcinoma stem cells. *Gastroenterology* 2014; **147**: 1393-404.

36 Won C, Kim BH, Yi EH et al. Signal transducer and activator of transcription 3-mediated CD133 up-regulation contributes to promotion of hepatocellular carcinoma. *Hepatology* 2015; **62**: 1160-73.

37 Hiraoka Y, Ohno M, Yoshida K et al. Enhancement of alpha-secretase cleavage of amyloid precursor protein by a metalloendopeptidase nardilysin. *J Neurochem* 2007; **102**: 1595-605.

38 Kessler JH, Khan S, Seifert U et al. Antigen processing by nardilysin and thimet oligopeptidase generates cytotoxic T cell epitopes. *Nat Immunol* 2011; **12**: 45-53.

39 Gong G, Waris G, Tanveer R, Siddiqui A. Human hepatitis C virus NS5A protein alters intracellular calcium levels, induces oxidative stress, and activates STAT-3 and NF-kappa B. *Proc Natl Acad Sci U S A* 2001; **98**: 9599-604.

40 Waris G, Turkson J, Hassanein T, Siddiqui A. Hepatitis C virus (HCV) constitutively activates STAT-3 via oxidative stress: role of STAT-3 in HCV replication. *J Virol* 2005; **79**: 1569-80.

41 Machida K, Cheng KT, Lai CK, Jeng KS, Sung VM, Lai MM. Hepatitis C virus triggers mitochondrial permeability transition with production of reactive oxygen species, leading to DNA damage and STAT3 activation. *J Virol* 2006; **80**: 7199-207.

42 Yoshida T, Hanada T, Tokuhisa T et al. Activation of STAT3 by the hepatitis C virus

core protein leads to cellular transformation. *J Exp Med* 2002; **196**: 641-53.

43 Basu A, Meyer K, Lai KK et al. Microarray analyses and molecular profiling of Stat3 signaling pathway induced by hepatitis C virus core protein in human hepatocytes. *Virology* 2006; **349**: 347-58.

Figure legends

Fig. 1. NRDC is up-regulated in HCC tissue and serum NRDC is a prognostic marker for HCC patients with hepatitis C. (a) Immunohistochemistry for an anti-human NRDC mouse monoclonal antibody (#102). Scale bar represents 500 μm. (b, c) Western blotting for an anti-human NRDC mouse monoclonal antibody (#23) for tumor (T) and the adjacent non-tumor liver tissue (NT). The expression level of NRDC is quantified by densitometry and normalized to ß-actin. The expression levels of NT and T are converted to logarithms, which are compared using the paired t-test for each patient (n = 27). (d) Comparison of serum NRDC in healthy volunteers (n = 112) and HCC patients (n = 220). Data are expressed as a scatter plot and a box-and-whisker plot. The box, horizontal bar in the box, and whisker represent the interquartile range, median, and quartile to the outermost value within a 1.5 × interquartile range, respectively. Wilcoxon's test is used for statistical comparison. (e) Scatter plot of histological NRDC expression (tumor to non-tumor ratio) and serum NRDC in each patient (n = 27). Linear correlation is examined using Pearson's correlation analysis. (f, g, h) Kaplan-Meier curves of overall survival (f), recurrence-free survival (g), and survival after recurrence (h) related to the serum NRDC in patients with hepatitis C. The cutoff value is determined as 844.6 pg/ml by receiver operating characteristic analysis for the outcome

of death within 3 years of surgery among patients with hepatitis C. Cumulative survival rates are compared using the log-rank test.

Fig. 2. DEN-induced hepatocarcinogenesis is suppressed in NRDC-deficient mice. (a) Hepatocarcinogenesis is assessed by the tumor number (left lower graph) and maximum tumor size (right lower graph) for wild-type mice (*Nrdc* +/+, n = 15) and heterozygous NRDC-deficient mice (*Nrdc* +/-, n = 14). Data are expressed as the mean plus/minus the standard error, which are compared using the unpaired t-test. Arrowheads indicate tumors. Scale bar represents 10 mm. (b) Immunohistochemistry for an anti-mouse NRDC rat monoclonal antibody (#135) in the mouse liver. Scale bar represents 100 μm. (c) Immunohistochemistry for Ki67 in the mouse liver. The number of total and Ki67-positive cells is counted for 5 random high-power fields per mouse. Data are expressed as the mean plus/minus the standard error of the proportion of Ki67-positive cells of 5 mice per each genotype, which are compared using the unpaired t-test. Scale bar represents 200 μm for large panels and 50 μm for small panels.

Fig. 3. Gene knockdown of NRDC suppresses spheroid growth and STAT3 phosphorylation in HCC cells. (a, b) Multicellular spheroid growth assay in 96-well

ultra-low attachment plates for HCC cell lines, Huh-7 (a) and Hep3B (b). Seeding densities are 1,000 cells and 2,500 cells for Huh-7 and Hep3B cells, respectively. Volume index represents the $S^{1.5}$ [S = sectional area of the spheroid (×10,000 μm^2)]. Representative data from 3 independent experiments are shown. Data are expressed as the mean plus/minus the standard error of 6 wells, which are compared using the unpaired t-test (*P< 0.05, **P< 0.01, ***P<0.001). Scale bar represents 100 μm. (c) Western blotting of spheroid-derived protein from Huh-7 cells. Expression levels of phosphorylated proteins and ß actin are quantified by densitometry, and the mean expression ratio and 95% confidence interval of knockdown cells to control cells of 5 independent experiments are described. Asterisks (*) represent that the 95% confidence interval does not cross 1.0.

Fig. 4. Effect of STAT3 inhibition on spheroid growth. (a) Western blotting of spheroid-derived protein from Huh-7 cells. (b) Spheroid growth assay for Huh-7 cells. Seeding density is 1,000 cells. Representative data from 3 independent experiments are shown. Data are expressed as the mean plus/minus the standard error of 6 wells, which are compared using the unpaired t-test (*P< 0.05, **P< 0.01, ***P<0.001). Scale bar represents 100 μm. (c) Spheroid growth inhibition with S3I-201. One-thousand Huh-7

cells were incubated with 36 μM of S3I-201 (STAT3 inhibitor) or equivalent amounts of DMSO for 7 days in 96-well ultra-low attachment plates. Data are expressed as the mean plus/minus the standard error of 5 independent experiments, which are compared using the unpaired t-test (** $P < 0.01$, N.S: not significant). Scale bar represents 100 μm.

List of Supporting Information

Fig. S1. Kaplan-Meier curves of overall survival (a), recurrence-free survival (b), and survival after recurrence (c) related to the serum NRDC for all patients. The cutoff value is determined as 780.7 pg/ml by receiver operating characteristic analysis for the outcome of death within 3 years of surgery among all patients. Cumulative survival rates are compared using the log-rank test.

Fig. S2. Survival analysis related to the NRDC gene expression level in HCC tissue obtained from The Cancer Genome Atlas (TCGA) RNA-seq database. (a) Histogram of NRDC gene expression levels in 370 patients. FPKM-UQ of the NRDC gene expression level is log2-transformed. (b) Kaplan-Meier curve of overall survival related to the NRDC gene expression level. CART technique determines the cutoff point as 11.881 of the log2-transformed FPKM-UQ of the NRDC gene expression level. Cumulative survival rates are compared using the log-rank test. FPKM-UQ: upper quartile fragments per kilobase of exon per million reads mapped, CART: classification and regression tree

Table S1. List of primary antibodies for western blotting.

Table S2. Demographics of all patients.

Table 1. Demographics of patients with hepatitis C.

	NRDC-low (N = 55)	NRDC-high (N = 65)	*P* value
Age ≥/< 65	33/22	41/24	0.730
Sex M/F	43/12	53/12	0.647
HBs-antigen (+)	3 (5.5%)	1 (1.5%)	0.228
Child-Pugh A/B	50/5	60/5	0.783
Liver cirrhosis	22 (40.0%)	27 (41.5%)	0.864
α-fetoprotein >/≤ 400 ng/ml	16/39	17/48	0.720
Single/multiple tumor	34/21	33/32	0.224
Tumor size > 3 cm	29 (52.7%)	48 (73.9%)	0.016
Vascular invasion (+)	25 (45.5%)	36 (55.4%)	0.278
Extrahepatic metastasis (+)	0 (0%)	4 (6.2%)	0.025
Poor differentiation	13 (23.6%)	17 (27.0%)	0.677

The cutoff value is 844.6 pg/ml. Liver cirrhosis is confirmed by pathological examination of the resected specimens. Differentiation was unknown in 2 patients because of tumor necrosis.

HBs-antigen: hepatitis B surface antigen

Table 2. Cox proportional hazard model for overall survival for patients with hepatitis C.

	HR	95% CI	*P* value
Multiple tumor	1.56	1.00-2.43	0.049
Vascular invasion (+)	1.94	1.25-3.04	0.003
Liver cirrhosis	2.05	1.31-3.22	0.002
Serum NRDC ≥ 844.6 pg/ml	1.92	1.23-3.03	0.004

Patients with 30-day mortality or extrahepatic metastasis are excluded from this analysis. Since large tumor size (> 3cm) is correlated with high serum NRDC, tumor size is not submitted to this multivariate analysis as an independent variable.

HR: hazard ratio, CI: confidence interval

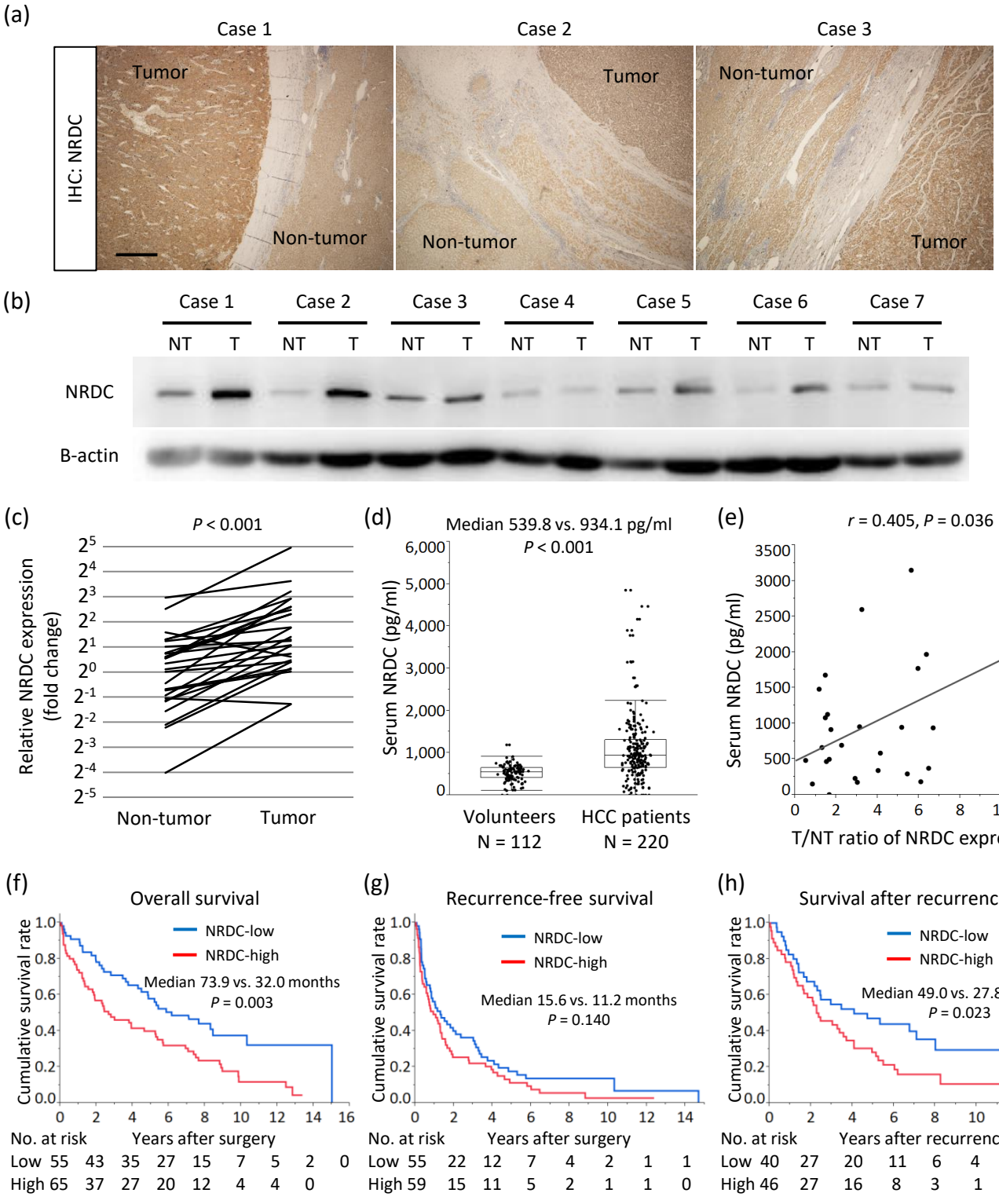
(a)
Case 1
Case 2
Case 3
IHC: NRDC
Tumor
Non-tumor
Tumor
Non-tumor
Non-tumor
Tumor
(b)
Case 1
Case 2
Case 3
Case 4
Case 5
Case 6
Case 7
NT
T
NRDC
B-actin
(c)
P < 0.001
Relative NRDC expression (fold change)
Non-tumor
Tumor
(d)
Median 539.8 vs. 934.1 pg/ml
P < 0.001
Serum NRDC (pg/ml)
Volunteers
N = 112
HCC patients
N = 220
(e)
r = 0.405, P = 0.036
Serum NRDC (pg/ml)
T/NT ratio of NRDC expression
(f)
Overall survival
NRDC-low
NRDC-high
Median 73.9 vs. 32.0 months
P = 0.003
Cumulative survival rate
No. at risk
Years after surgery
Low 55 43 35 27 15 7 5 2 0
High 65 37 27 20 12 4 4 0
(g)
Recurrence-free survival
NRDC-low
NRDC-high
Median 15.6 vs. 11.2 months
P = 0.140
Cumulative survival rate
No. at risk
Years after surgery
Low 55 22 12 7 4 2 1 1
High 59 15 11 5 2 1 1 0
(h)
Survival after recurrence
NRDC-low
NRDC-high
Median 49.0 vs. 27.8 months
P = 0.023
Cumulative survival rate
No. at risk
Years after recurrence
Low 40 27 20 11 6 4 1 0
High 46 27 16 8 3 1 0

Fig. 1

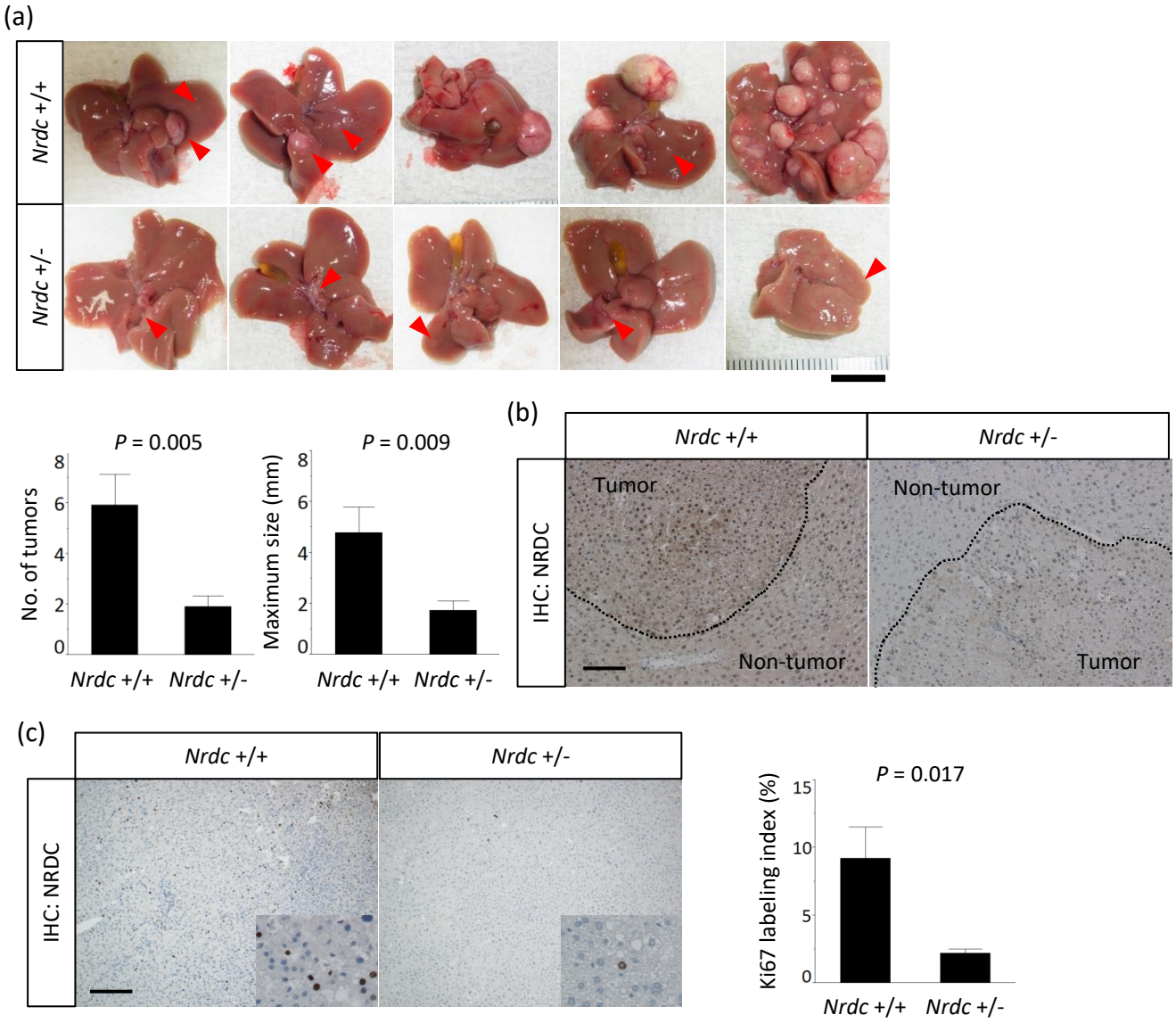
(a)
Nrdc +/+
Nrdc +/-
P = 0.005
No. of tumors
Nrdc +/+
Nrdc +/-
P = 0.009
Maximum size (mm)
Nrdc +/+
Nrdc +/-
(b)
Nrdc +/+
Nrdc +/-
IHC: NRDC
Tumor
Non-tumor
Non-tumor
Tumor
(c)
Nrdc +/+
Nrdc +/-
IHC: NRDC
P = 0.017
Ki67 labeling index (%)
Nrdc +/+
Nrdc +/-

Fig. 2

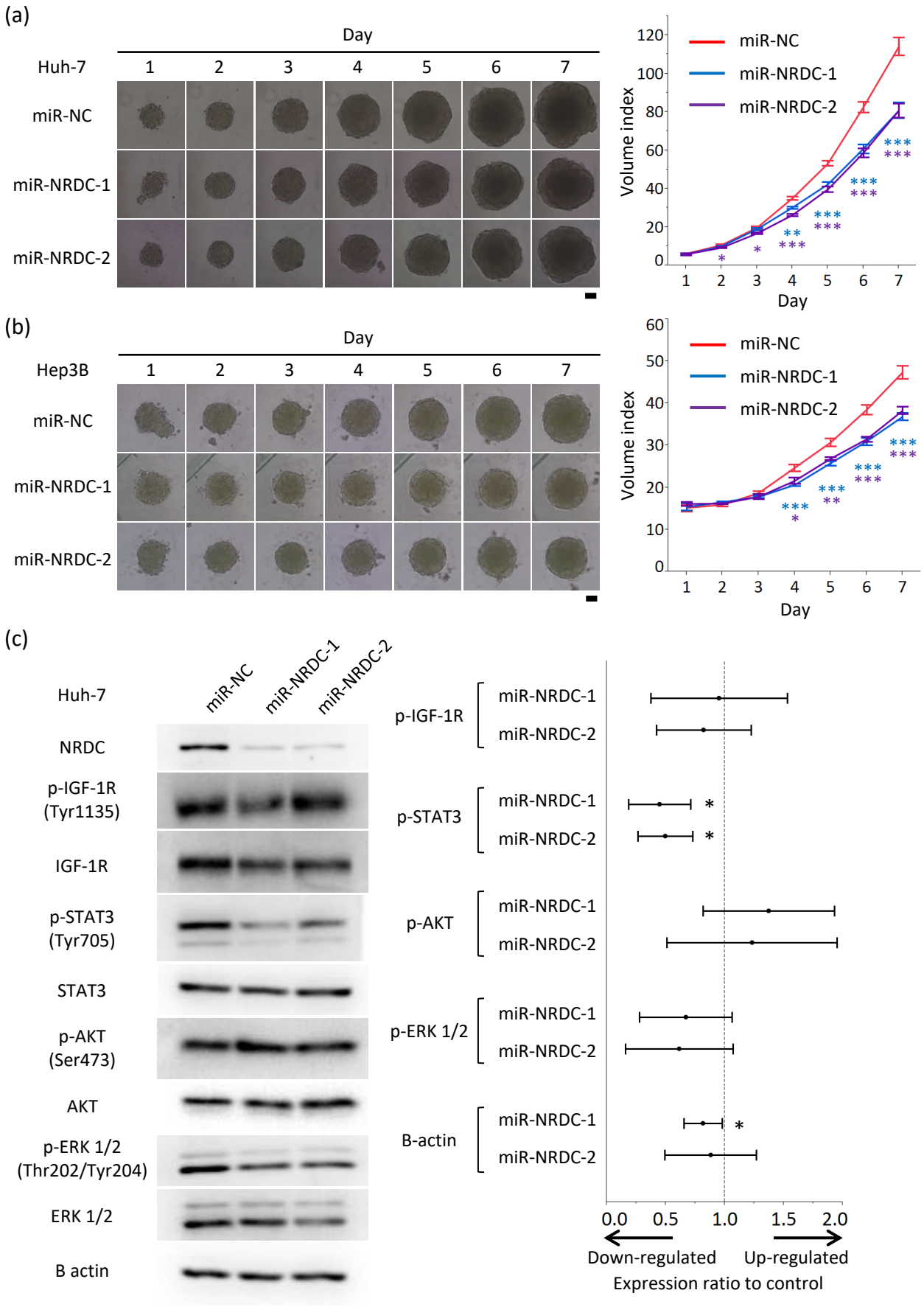
(a)
Day
Huh-7
1
2
3
4
5
6
7
miR-NC
miR-NRDC-1
miR-NRDC-2
Volume index
Day
(b)
Hep3B
(c)
NRDC
p-IGF-1R (Tyr1135)
IGF-1R
p-STAT3 (Tyr705)
STAT3
p-AKT (Ser473)
AKT
p-ERK 1/2 (Thr202/Tyr204)
ERK 1/2
B actin
p-IGF-1R
p-STAT3
p-AKT
p-ERK 1/2
B-actin
Down-regulated
Up-regulated
Expression ratio to control

Fig. 3

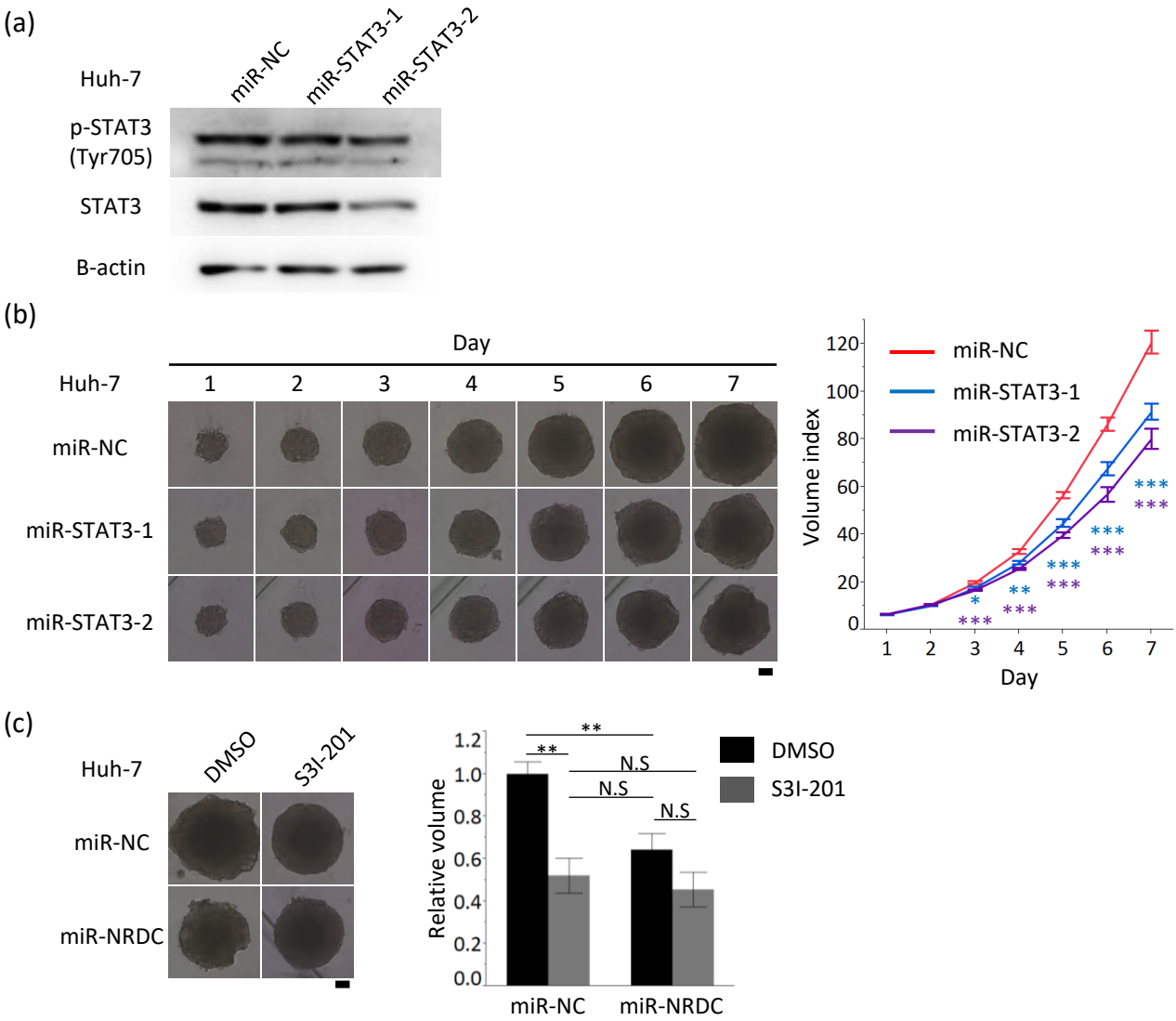
(a)
Huh-7
miR-NC
miR-STAT3-1
miR-STAT3-2
p-STAT3
(Tyr705)
STAT3
B-actin
(b)
Day
Huh-7
1
2
3
4
5
6
7
miR-NC
miR-STAT3-1
miR-STAT3-2
Volume index
120
100
80
60
40
20
0
Day
(c)
Huh-7
DMSO
S3I-201
miR-NC
miR-NRDC
Relative volume
1.2
1.0
0.8
0.6
0.4
0.2
0.0
**
**
N.S
N.S
N.S
DMSO
S3I-201
miR-NC
miR-NRDC

Fig. 4

Table S1. List of primary antibodies for western blotting

Target of primary antibody	Source	Dilution	Dilution reagent
Human NRDC #23	Established in our laboratory	1:2000	T-PBS
ß-actin	SC	1:000	T-PBS
AKT	CST	1:1000	5% BSA in T-PBS
ERK 1/2	CST	1:1000	5% BSA in T-PBS
IGF-1R	CST	1:1000	5% BSA in T-PBS
STAT3	CST	1:1000	5% BSA in T-PBS
Phospho-AKT (Ser473)	CST	1:1000	Can Get Signal 1
Phospho-ERK 1/2 (Thr202/Tyr204)	CST	1:1000	Can Get Signal 1
Phospho-IGF-1R (Tyr1135)	CST	1:1000	Can Get Signal 1
Phospho-STAT3 (Tyr705)	CST	1:1000	Can Get Signal 1

Can Get Signal was obtained from Toyobo, Osaka, Japan

BSA: bovine serum albumin, obtained from Wako, Osaka, Japan

CST: Cell Signaling Technology (CST), Danvers, MA, USA

SC: SantaCruz, Biotechnology Dallas, USA

Table S2. Demographics of all patients

	NRDC-low (N=82)	NRDC-high (N=138)	*P* value
Age ≥/< 65	43/39	77/61	0.629
Sex M/F	63/19	112/26	0.444
HBs-antigen (+)	17 (20.7%)	28 (20.3%)	0.937
HCV-antibody (+)	48 (58.5%)	72 (52.2%)	0.359
Child-Pugh A/B	78/4	127/11	0.368
Liver cirrhosis	28 (34.2%)	40 (29.0%)	0.425
α-fetoprotein >/≤ 400 ng/ml	19/63	45/93	0.132
Single/multiple tumor	45/37	78/60	0.812
Tumor size > 3cm	51 (62.2%)	104 (75.4%)	0.040
Vascular invasion (+)	40 (48.8%)	72 (52.2%)	0.626
Extrahepatic metastasis (+)	1 (1.2%)	8 (5.8%)	0.071
Poor differentiation	18 (22.0%)	36 (26.7%)	0.433

The cutoff value is 780.7 pg/ml. Liver cirrhosis is confirmed by pathological examination of the resected specimens. Differentiation was unknown in 3 patients because of the tumor necrosis.

HBs-antigen: hepatitis B surface antigen, HCV-antibody: hepatitis C virus antibody

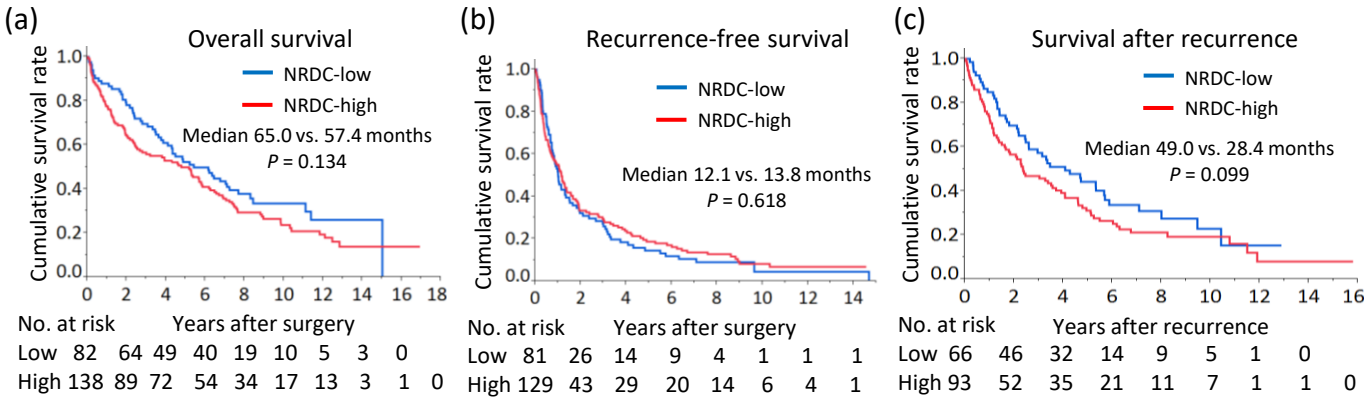

Fig. S1. Kaplan-Meier curves of overall survival (a), recurrence-free survival (b), and survival after recurrence (c) related to the serum NRDC for all patients. The cutoff value is determined as 780.7 pg/ml by receiver operating characteristic analysis for the outcome of death within 3 years of surgery among all patients. Cumulative survival rates are compared using the log-rank test.

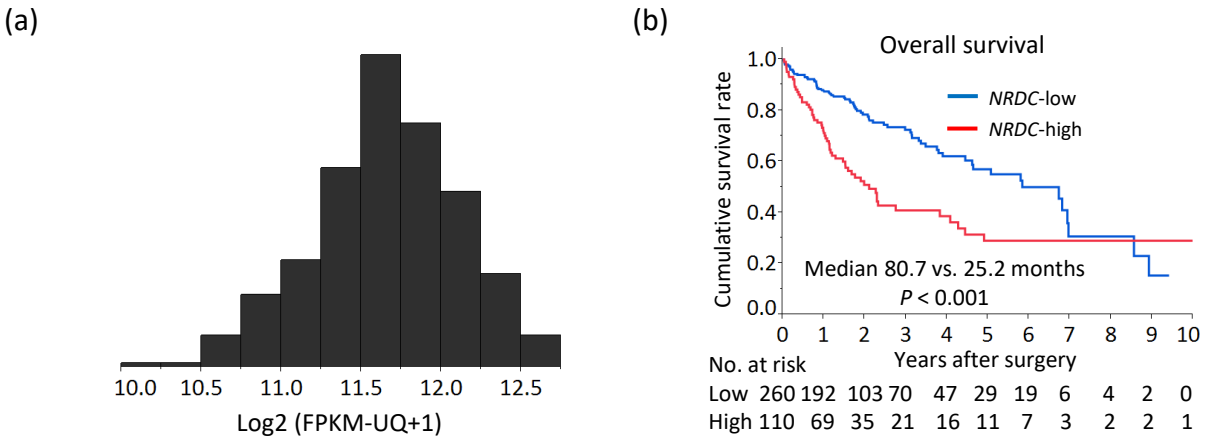

Fig. S2. Survival analysis related to the NRDC gene expression level in HCC tissue obtained from The Cancer Genome Atlas (TCGA) RNA-seq database. (a) Histogram of NRDC gene expression levels in 370 patients. FPKM-UQ of the NRDC gene expression level is log2-transformed. (b) Kaplan-Meier curve of overall survival related to the NRDC gene expression level. CART technique determines the cutoff point as 11.881 of the log2-transformed FPKM-UQ of the NRDC gene expression level. Cumulative survival rates are compared using the log-rank test. FPKM-UQ: upper quartile fragments per kilobase of exon per million reads mapped, CART: classification and regression tree